NADH-regulated metabolic model for growth of Methylosinus trichosporium OB3b. Model presentation, parameter estimation, and model validation

Sipkema, E.M; de Koning, W.; Ganzeveld, K.J; Janssen, D.B.; Beenackers, A.A C M

Published in:
Biotechnology Progress

DOI:
10.1021/bp9901567

NADH-Regulated Metabolic Model for Growth of *Methylosinus trichosporium* OB3b. Model Presentation, Parameter Estimation, and Model Validation

E. Marijn Sipkema,[†] Wim de Koning,[‡] Klaassien J. Ganzeveld,*[,†] Dick B. Janssen,[‡] and Antonie A. C. M. Beenackers[†]

Chemical Engineering and Biochemistry Departments, University of Groningen, NL-9747 AG Groningen, The Netherlands

A biochemical model is presented that describes growth of *Methylosinus trichosporium* OB3b on methane. The model, which was developed to compare strategies to alleviate NADH limitation resulting from cometabolic contaminant conversion, includes (1) catabolism of methane via methanol, formaldehyde, and formate to carbon dioxide; (2) growth as formaldehyde assimilation; and (3) storage material (poly-β-hydroxybutyric acid, PHB) metabolism. To integrate the three processes, the cofactor NADH is used as central intermediate and controlling factor—instead of the commonly applied energy carrier ATP. This way a stable and well-regulated growth model is obtained that gives a realistic description of a variety of steady-state and transient-state experimental data. An analysis of the cells' physiological properties is given to illustrate the applicability of the model. Steady-state model calculations showed that in strain OB3b flux control is located primarily at the first enzyme of the metabolic pathway. Since no adaptation in V_{MAX} values is necessary to describe growth at different dilution rates, the organism seems to have a "rigid enzyme system", the activity of which is not regulated in response to continued growth at low rates. During transient periods of excess carbon and energy source availability, PHB is found to accumulate, serving as a sink for transiently available excess reducing power.

Introduction

Chlorinated ethenes, such as the environmental pollutant trichloroethene, can be converted aerobically only via cometabolism. In this process, conversion results from the nonspecificity of oxygenating enzymes. Expression of these enzymes occurs during growth on compounds such as alkanes, aromatics, and ammonia. Specific for all oxygenases is the insertion of molecular oxygen, which requires reducing equivalents. Usually, the reductants are supplied by NADH (reduced nicotinamide adenine dinucleotide). In cometabolic conversions the initial hydroxylation products cannot be metabolized further. Therefore, the cofactor NADH is not regenerated, and a net NADH consumption results. To continue the contaminant conversion, NADH needs to be regenerated by metabolism of other substrates.

To evaluate the effect of different strategies to regenerate NADH, a model was developed. In a cell, NADH plays a central role, both in the energy-transforming and oxidation−reduction reactions and in the metabolic regulation processes (*1*−*5*). Therefore, in the model all three processes of catabolism, biosynthesis, and PHB metabolism are incorporated, and NADH is used as the integrating and controlling factor. PHB metabolism is included because storage material can act as an endogenous electron donor (*6*, *7*). Up till now, modeling studies based on the metabolic pathways focused mainly on the energy carrier ATP (adenosine triphosphate) (*8*−*11*). Although for energy-consuming processes this is certainly the best choice, processes in which NADH plays a prominent role like the cometabolic conversions might better be described by using NADH as principal regulator.

This contribution presents a metabolic model developed for *Methylosinus trichosporium* OB3b, an organism selected for its characteristics of cometabolic contaminant conversion. The model describes growth of strain OB3b on methane in a continuous culture at various dilution rates and the metabolic responses of the organism to pulses of the intermediates methanol, formaldehyde, and formate. Issues such as parameter sensitivity, parameter estimation, and model validation are addressed. Characteristics of the model and their relation to physiological properties of the organism such as flux control and growth regulation are discussed. In the following article, the growth model is extended to incorporate cometabolic contaminant conversion.

Materials and Methods

M. trichosporium OB3b was grown continuously at a dilution rate (D) of 0.024 h^{-1} or 0.048 h^{-1} in a 3-L bioreactor as described by Sipkema et al. (*13*) (experimental setup, analysis, and procedures) and (*14*) (medium composition), with methane as the sole carbon source. Copper limitation was maintained to ensure expression of soluble methane monooxygenase (sMMO), an oxygenating enzyme with very good characteristics for cometabolic contaminant conversion. To prevent light-

* Tel: (31)-(0)50-3634333. Fax: (31)-(0)50-3634479. E-mail: K.J.Ganzeveld@chem.rug.nl.
[†] Chemical Engineering Department.
[‡] Biochemistry Department.

10.1021/bp9901567 CCC: $19.00
Published on Web 03/03/2000

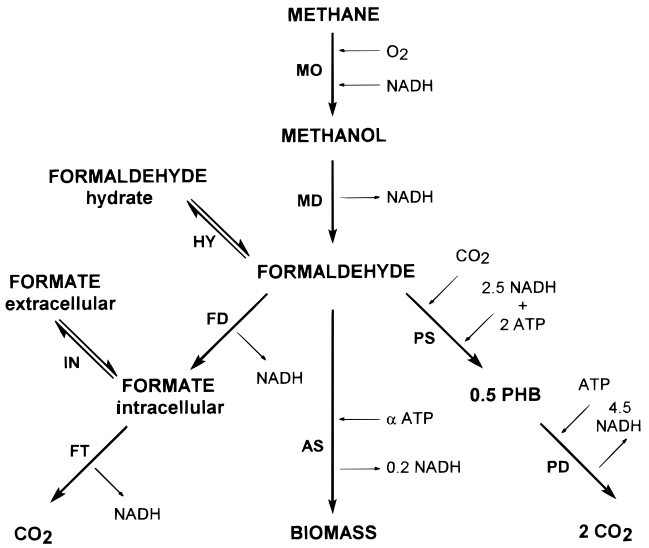

Figure 1. Steps incorporated in the metabolic model for growth of *M. trichosporium* OB3b on methane. The stoichiometry is included; NAD, ADP, H_2O, and HNO_3 are not shown.

induced inactivation, continuous cultures were protected from light. Dissolved oxygen was monitored online, with data collection in a computer. Routinely, samples were taken and analyzed for biomass concentration (*14*). During transient-state experiments, samples were quenched immediately after being taken and analyzed for PHB and NAD(H) levels (PHB, H_3PO_4; NAD, HCl; NADH, NaOH; all end concentrations of 0.1 M). Oxygen and methane concentrations in the gas inlet and outlet were measured by gas chromatography.

Experiments. Transient-state experiments were performed, starting from steady-state, by (1) blocking the inlet gas flow of methane and air during a short period of time (min) (gas block experiment); (2) injecting a pulse of dissolved methanol, formaldehyde, or formate (0.01−1 mM end concentration) (pulse experiment) (see ref 13); and (3) changing the concentration of methanol in the medium inlet from 0 to 25 or 50 mM during a limited period of time (min) (step experiment).

Analysis. PHB concentrations (wt %) were determined fluorometrically as described by Degelau et al. (*15*). A calibration curve was obtained via parallel analysis of samples using the technique of van Aalst-van Leeuwen et al. (*16*). NADH concentrations were determined following the fluorometric method described by Matin and Gottschal (*4*). Intracellular concentrations were calculated using a cell volume of 1.7 μL mg^{-1} (*17*). Time-dependent model calculations were carried out using the Episode routine of the software program Scientist (Micromath Inc., Salt Lake City, UT). Steady-state solutions were verified with Mathcad version 5$^+$ (MathSoft Inc., Cambridge, MA).

Model Development

System Definition. The model for growth of *M. trichosporium* OB3b on methane includes all metabolic steps involving NADH and similar compounds that may become rate-limiting under relevant experimental conditions. However, for reasons of simplicity and clearness not all physiological aspects of the cell, like the TCA cycle, will be discussed. Per step, a single enzyme or several enzymes may be involved. The following steps were incorporated (Figure 1) (*18*−*20*): methane conversion to methanol, mediated by sMMO (MO) and requiring both molecular oxygen and NADH; methanol conversion to formaldehyde, mediated by methanol dehydrogenase (MD); and formaldehyde conversion via three different routes, (1) to formate via formaldehyde dehydrogenase (FD) and then to carbon dioxide via formate dehydrogenase (FT) (catabolism); (2) to biomass, which occurs via the serine pathway (biosynthesis or assimilation, AS); and finally, (3) to PHB (PHB synthesis, PS) and then to carbon dioxide (PHB degradation, PD). So, formaldehyde acts as a central intermediate.

All of the catabolic steps, from methane down to carbon dioxide, are assumed to involve NADH. Although this is correct for the conversion of formate and probably formaldehyde (*19*, *21*, *22*), it is a simplification of the situation for methanol dehydrogenase. This enzyme actually involves PQQH (reduced pyrrolo-quinoline quinone), which cannot be used as a cofactor by the sMMO enzyme (*18*, *23*). However, like NADH, PQQH is oxidized in the electron transport chain and thus leads to energy production. Since for NADH the energy or ATP function is the most important property (*24*), PQQH can be substituted by NADH in the model. Furthermore, for simplicity both cofactors are assumed to produce an equal amount of energy, although PQQH enters the electron transport chain at a lower level than NADH (level of cytochrome *c* (*18*)). Model calculations show that incorporation of this discrepancy, by assuming only 1 ATP (cytochrome *c*) to be produced instead of 3 ATP (NADH), does not significantly influence the model predictions (see Results). This indicates that the model is not sensitive to the discrepancy and no simulation errors will originate from this assumptiom.

PHB, the only storage material taken into account, is formed via a cyclic pathway originating at acetyl-CoA (*25*). By separating PHB formation from biomass synthesis (Figure 1), growth that occurs as a result of breakdown of PHB via the serine pathway intermediate, acetyl-CoA, is neglected. This description is realistic, since biomass is synthesized from C_3 compounds only (primarily 3-phosphoglycerate) (*26*, *27*), whereas the C_2 compounds (acetyl-CoA) are used for fat metabolism (*20*). A similar assumption was made by Williams (*28*) on the basis of detailed studies of enzymes related to PHB metabolism of strain OB3b.

Production of NADH as a result of PHB degradation via acetyl-CoA to carbon dioxide (PD, Figure 1), the main role of PHB according to Williams (*28*), is incorporated in the model. However, unless growth conditions are unbalanced as during transient-state experiments, this breakdown is not expected to occur at a measurable rate, because dissimilation of formaldehyde via formate to carbon dioxide is energetically more favorable. In diluted aquatic solutions, this formaldehyde is present mostly in its hydrated form (*29*). Therefore, a distinction is made between formaldehyde hydrate and formaldehyde (HY, Figure 1). Only the latter is a substrate for formaldehyde dehydrogenase.

Many compounds cannot cross the cellular membrane freely, and under certain conditions transport can become rate-limiting. In the model for strain OB3b, this was assumed to be the case for formate (IN, Figure 1). All other compounds incorporated in the model are assumed to cross freely, except for NAD(H), PHB, and formaldehyde, which are considered within the cell only (Table 1).

Stoichiometry. The stoichiometry of the conversion reactions is based on the metabolic pathways. Thus, methane conversion to methanol is described by

$$CH_4 + O_2 + NADH_2 \rightarrow CH_3OH + H_2O + NAD \quad (1)$$

Table 1. Compounds Incorporated in the Model for Growth of *M. trichosporium* OB3b on Methane

location	compound	abbrev	concn
	biomass	X	C_X
intracellular	NAD	n	C_n
	NADH	nh	C_{nh}
	PHB	b	C_b
	formaldehyde	fd	C_{fd}
	formate	ft	C_{ft}
averaged over intra- and extracellular	methane	m	$C_{L,m}$
	methanol	ml	$C_{L,ml}$
	fd hydrate	fd	$C_{L,fd}$
	formate	ft	$C_{L,ft}$
	oxygen	o	$C_{L,o}$

where the correct stoichiometry is introduced for NADH. Similarly, methanol conversion to formaldehyde (with PQQ(H)═NAD(H)), formaldehyde conversion to formate, and formate conversion to carbon dioxide, are described by, respectively

$$CH_3OH + NAD \rightarrow H_2CO + NADH_2 \quad (2)$$

$$H_2CO + H_2O + NAD \rightarrow H_2CO_2 + NADH_2 \quad (3)$$

$$H_2CO_2 + NAD \rightarrow CO_2 + NADH_2 \quad (4)$$

For synthesis of PHB (═$C_4H_6O_2$), formaldehyde is first converted in the serine pathway to acetyl-CoA (═C_2H_3O−SCoA) (*18*):

$$H_2CO + CO_2 + 2ATP + 2NADH_2 + CoASH \rightarrow C_2H_3O{-}SCoA + 2H_2O + 2NAD + 2ADP + 2\tilde{}P \quad (5)$$

where ADP is adenosine diphosphate and ~P is a phosphate group. Acetyl-CoA is then converted to PHB (*25*):

$$C_2H_3O{-}SCoA + 0.5NADH_2 \rightarrow 0.5C_4H_6O_2 + CoASH + 0.5NAD \quad (6)$$

where NADPH is pooled with NADH (*30*). PHB is converted, via acetoacetate, to acetyl-CoA again (cyclic pathway) (*25*):

$$C_4H_6O_2 + 2ATP + 2CoASH + NAD \rightarrow 2\,C_2H_3O{-}SCoA + NADH_2 + 2ADP + 2\tilde{}P \quad (7)$$

If not converted to PHB (eq 6), acetyl-CoA is degraded via the tricarboxylic acid cycle to carbon dioxide:

$$C_2H_3O{-}SCoA + 3H_2O + 4NAD \rightarrow 2CO_2 + 4NADH_2 + CoASH \quad (8)$$

Growth of *M. trichosporium* OB3b is described as formaldehyde assimilation:

$$H_2CO + \alpha ATP + 0.2HNO_3 + 0.2NAD \rightarrow CH_{1.8}O_{0.5}N_{0.2} + 0.55O_2 + 0.2NADH_2 + \alpha ADP + \alpha\tilde{}P \quad (9)$$

where α is the amount of energy (mol ATP) used per C-mole of biomass formed, $CH_{1.8}O_{0.5}N_{0.2}$ is the standard biomass composition (*31*), NO_3^- is taken as the nitrogen source, and the oxygen term on the right-hand side is included to express the difference in oxygen content between substrate and product (O_2 is not produced). Equation 9 is a simplification, since assimilation of biomass via the serine pathway involves carbon dioxide fixation. The approach is therefore only valid under conditions in which carbon dioxide is available in excess. However, in practice, carbon dioxide will be produced sufficiently from the dissimilation of formaldehyde. Only when hydrogen gas is used as an additional energy source might this be problematic.

The ATP consumed in the reactions above is formed from NADH by oxidative phosphorylation according to

$$NADH_2 + 0.5O_2 + \delta ADP + \delta\tilde{}P \rightarrow \delta ATP + H_2O + NAD \quad (10)$$

where δ, the P/O ratio, is the efficiency of this conversion.

In the model, two conservation quantities are taken into account, the sum of pyridine nucleotides (NAD(H)) and that of the adenosine nucleotides (ADP, ATP). As an example, for NAD(H)

$$n_{tot} = NAD + NADH_2 \quad (11)$$

where n_{tot}, the sum of NAD and NADH, is a constant.

Kinetics. Substrate conversion for each step incorporated in the model (Figure 1) is described according to Michaelis−Menten kinetics, with a separate term per (co)substrate that may become rate-limiting. Thus, methane conversion by sMMO is described as

$$q_{MO} = V_{MAX,MO}\left(\frac{C_{L,m}}{C_{L,m} + K_{M,MO,m}}\right)\left(\frac{C_{nh}}{C_{nh} + K_{M,MO,nh}}\right)\left(\frac{C_{L,o}}{C_{L,o} + K_{M,MO,o}}\right) \quad (12)$$

with q_i the specific conversion rate and $V_{MAX,i}$ the maximum specific conversion rate of the sMMO (i = MO) [mol s^{-1} kg^{-1}], $K_{M,i,j}$ the affinity constant of the sMMO for compound j, with j = m (methane), j = nh (NADH), j = o (oxygen) [mol L^{-1}], $C_{L,j}$ the overall and C_j the intracellular compound concentration [mol L^{-1}]. For PHB metabolism, more complex equations are used. These equations are based on enzyme kinetics, ensure realistic behavior, and prevent model instabilities.

To describe the rapid formation of PHB that results from only a modest increase in NADH (*6*, *32*), the Hill equation (*33*) is used for the PHB synthesis rate q_{PS}:

$$q_{PS} = V_{MAX,PS}\left(\frac{C_{fd}}{C_{fd} + K_{M,PS,fd}}\right)\left(\frac{C_{nh}^p}{C_{nh}^p + K_{M,PS,nh}^p}\right) \quad (13)$$

where C_{fd} is the (intracellular) formaldehyde concentration [mol L^{-1}], and p is the power in the Hill term. Depending on the amount of information available on the physiology and enzyme levels, other descriptions of PHB synthesis can be incorporated, e.g., as recently presented by van Aalst-van Leeuwen et al. (*16*) for *P. pantotrophus* and by Leaf and Srienc (*34*) for *A. eutrophus*.

For breakdown of PHB, q_{PD}, an equation is used which ensures the expected negligible PHB turnover under steady-state conditions (*6*), while enabling PHB mobilization at very low NADH levels (*6*, *28*, *32*):

$$q_{PD} = V_{MAX,PD}\left(\frac{C_b}{C_b + K_{M,PD,b}}\right)\left(\frac{C_n}{C_n + K_{M,PD,n}}\right)\left(\frac{C_{L,o}}{C_{L,o} + K_{M,PD,o}}\right)\left(\frac{1}{1 + \frac{C_{nh}}{K_{I,PD,nh}}}\right) \quad (14)$$

with the subscripts b = PHB, n = NAD, and using for the inhibition constant $K_{I,PD,nh}$ [mol L^{-1}]:

$$K_{I,PD,nh} = K_{I,PD,MAX}\left(1 - \frac{C_{nh}^{w}}{C_{nh}^{w} + K_{M,PD,SP}^{w}}\right) + K_{I,PD,MIN}\left(\frac{C_{nh}^{w}}{C_{nh}^{w} + K_{M,PD,SP}^{w}}\right) \quad (15)$$

with w the power in the Hill term. If the NADH concentration is high ($C_{nh} \rightarrow C_{ntot}$), $K_{I,PD,nh}$ equals $K_{I,PD,MIN}$, the minimum K_I resulting in a maximal inhibition of PHB breakdown by NADH and thus a minimal decrease in PHB levels (eq 14). Inversely, if $C_{nh} \rightarrow 0$, $K_{I,PD,nh} \approx K_{I,PD,MAX}$ (eq 15), a minimal NADH-dependent inhibition occurs, and thus the rate of PHB breakdown is maximal (eq 14). When NADH levels drop below a certain set point ($= K_{M,PD,SP}$), the breakdown of PHB is induced to a degree depending on the value of the power w.

The rate of formaldehyde dehydration (v_{HY} [mol s^{-1} L^{-1}]) is assumed to be first-order and is described by rate constant k_{HY} [s^{-1}] and equilibrium constant $K_{EQ,fd}$ ($= C_{fd}/C_{L,fd}$, with $C_{L,fd}$ the concentration of formaldehyde hydrate). A first-order description was chosen to minimize the complexity of the model. As we could not measure it, this was the simplest approach to the phenomena. Transport of formate across the cellular membrane is incorporated as a fully reversible enzymatic reaction. Therefore, according to Segel (*33*), the net specific transport rate q_{IN} is

$$q_{IN} = \frac{V_{MAX,IN}\left(C_{L,ft}\frac{C_{ft}}{K_{EQ,ft}}\right)}{C_{L,ft} + K_{M,IN} + \frac{K_{M,IN}}{K_{M,EX}}C_{ft}} \quad (16)$$

with the subscript ft = formate, the subscripts IN and EX denoting the transport reactions directed intra- and extracellularly, respectively, and $K_{EQ,ft}$ the equilibrium constant of the reaction ($= C_{ft}/C_{L,ft}$).

Finally, under growth conditions (specific growth rate $\mu > 25\%\ \mu_{MAX}$), maintenance is neglected, while under conditions of prolonged absence of growth substrate, it is included with a rate q_M leading to NADH and oxygen consumption. In the appendix, a summary of all kinetic equations is given.

Model Simplification. Depending on the application considered, some substrate pools can be assumed to be in equilibrium. The concentrations of these compounds are then directly coupled to each other. If so, the number of parameters and the complexity of the model is reduced.

An aim of the growth model for strain OB3b was to describe NADH levels resulting from different dynamic feeding strategies. Alternatives for methane were methanol, formaldehyde, and formate. All of these substrates were therefore included in the model as dynamic pools, and their concentrations were allowed to vary as a function of time, as were the concentrations of PHB, biomass, and oxygen. Not included as dynamic pools were ATP and acetyl-CoA. As both components were not measured during the experiments, in contrast to PHB, biomass, and oxygen, we assume them to be in equilibrium with NADH and formaldehyde, respectively. This semi-steady-state approach is commonly used by well-known authors in the metabolic modeling area (*16*). It prevents needless complexity of the model.

Under the assumptions made, the reactions (eqs 5−10) were simplified by eliminating the ATP and acetyl-CoA levels, resulting in a single reaction for growth:

$$H_2CO + 0.2HNO_3 + (0.5\alpha/\delta - 0.55)O_2 + (\alpha/\delta - 0.2)NADH_2 \rightarrow CH_{1.8}O_{0.5}N_{0.2} + \alpha/\delta H_2O + (\alpha/\delta - 0.2)NAD \quad (17)$$

a single reaction for PHB synthesis:

$$H_2CO + CO_2 + (1/\delta)O_2 + (2.5 + 2/\delta)NADH_2 \rightarrow 0.5C_4H_6O_2 + (2 + 2/\delta)H_2O + (2.5 + 2/\delta)NAD \quad (18)$$

and, finally, a single reaction for PHB degradation:

$$C_4H_6O_2 + (1/\delta)O_2 + (6 - 2/\delta)H_2O + (9 - 2/\delta)NAD \rightarrow (9 - 2/\delta)NADH_2 + 4CO_2 \quad (19)$$

Substrate Concentrations. Substrate concentrations as a function of time follow from mass balances, which incorporate stoichiometry (eqs 1−4, 11, and 16−18) and enzyme kinetics (appendix), as well as reactor-specific mass transfer expressions (*13*). A distinction is made between overall concentrations such as for methane (averaged over intra- and extracellular, expressed in mol L^{-1} reactor volume), and intracellular concentrations such as for NADH (expressed in mol L^{-1} cell volume) (Table 1). Since PHB must always be formed by newly grown cells, in the mass balance for PHB, dilution resulting from growth is incorporated, whereas in the other intracellular balances it is not.

Parameter Estimation. The model contains a variety of parameters, which can be divided into reactor-specific variables (flows, volumes, mass transfer coefficients) (*13*) and organism-specific variables, including stoichiometric parameters (α, δ) and kinetic parameters (V_{MAX}, K_M).

Values for the organism-specific parameters were either taken from literature, determined in batch and cell-free extract measurements (Table 2), or fitted from steady-state and transient-state experimental data obtained with a single continuous culture grown at D = 0.048 h^{-1} (Table 3). The starting values for the fitting procedure were based on information available for similar enzymes and on assumptions concerning the influence of the limiting (co)substrate on the conversion rate. Either the (co)substrate controlled the conversion rate ($K_{M,j} \gg C_j$, $q = V_{MAX}\ C_j/K_M$, first-order in C_j), or it had no influence ($C_j \gg K_{M,j}$, $q = V_{MAX}$, zero-order in C_j). Further details concerning the fitting procedure are given below.

Results and Discussion

Sensitivity Analysis for Steady-State Conditions. Model calculations showed that only a small portion of the large number of affinity constants incorporated in the model (Tables 2 and 3) influence the steady-state biomass, PHB, and NADH concentrations determined (Table 4). Only those of the first enzyme (sMMO) and those at the branch point (FD, AS, PS; Figure 1) have a significant influence. The $K_{M,MO}$ values determine the amount of methane that enters the pathway (flux), and thus the steady-state biomass concentration. The NADH levels are not affected (Table 4), since $K_{M,MO,nh} \ll C_{nh}$ (Tables 2 and 3). Furthermore, because PHB synthesis is influenced primarily by these NADH levels (see eq 13, with $K_{M,PS,fd} \ll C_{fd}$, while $K_{M,PS,nh} \approx C_{nh}$ and $p = 5.2$), the PHB levels are not affected either (Table 4).

Table 2. Parameter Values of the Metabolic Model for Growth of *M. trichosporium* OB3b on Methane (part 1)[a]

enzyme system	parameter	value	source/type of experiment
sMMO	$V_{MAX,MO}$	6.1×10^{-3} mol s^{-1} kg^{-1}	Oldenhuis et al. (*35*)
	$K_{M,MO,m}$	0.037 mM	Sipkema et al. (*13*)
	$K_{M,MO,nh}$	0.050 mM	Fox et al. (*36*)
	$K_{M,MO,o}$	0.013 mM	Green and Dalton (*37*)
FD, FT	$V_{MAX,FT}$	0.013 mol s^{-1} kg^{-1}	cell-free extract measurement
	$K_{M,FT,ft}$	0.080 mM	Jollie and Lipscomb (*38*)
	$K_{M,FT,n}$	0.10 mM	Jollie and Lipscomb (*38*)
HY (fd)	k_{HY}	14 s^{-1}	batch experiments[b]
	$K_{EQ,fd}$	3.3×10^{-4}	Bieber and Trümpler (*39*) Walker (*29*)

[a] Parameters obtained from literature and determined in independent batch experiments. [b] Winkelman, J., unpublished results

Table 3. Parameter Values of the Metabolic Model for Growth of *M. trichosporium* OB3b on Methane (part 2)[a]

enzyme system	parameter	value	type of expt used for fitting
MD	$V_{MAX,MD}$	6.7×10^{-3} mol s^{-1} kg^{-1}	methanol pulse
	$K_{M,MD,ml}$	0.030 mM	methanol pulse
	$K_{M,MD,n}$	0.050 mM	methanol pulse
AS	$V_{MAX,AS}$	3.3 mol s^{-1} kg^{-1}	steady-state
	$K_{M,AS,fd}$	2.0×10^{-4} mM	formate pulse
	$K_{M,AS,nh}$	0.60 mM	formate pulse
	α	12	steady-state
	δ	2.0	assumption
FD	$V_{MAX,FD}$	3.0 mol s^{-1} kg^{-1}	formaldehyde pulse
PS	$V_{MAX,PS}$	1.4×10^{-3} mol s^{-1} kg^{-1}	steady-state
	$K_{M,PS,nh}$	3.0 mM	formate pulse
	p	5.2	formate pulse
IN (ft)	$V_{MAX,IN}$	1.0×10^{-3} mol s^{-1} kg^{-1}	formate pulse
	$K_{EQ,ft}$	1.0	formate pulse
	$K_{M,IN}$	0.010 mM	formate pulse
	$K_{M,EX}$	1.0 M	formate pulse
M	M	5.0×10^{-4} mol s^{-1} kg^{-1}	gas block
	$K_{M,M,nh}$	0.02 mM	gas block
	$K_{M,M,o}$	0.1 mM	gas block
PD[b]	$V_{MAX,PD}$	1.4×10^{-4} mol s^{-1} kg^{-1}	NADH limitation
	$K_{M,PD,b}$	1.0 mM	NADH limitation
	$K_{M,PD,SP}$	0.015 mM	NADH limitation
	$K_{I,PD,MAX}$	4.1×10^{-4} mM	NADH limitation
	$K_{I,PD,MIN}$	1.0×10^{-8} mM	NADH limitation
	w	10	NADH limitation

[a] Parameter set fitted from steady-state and transient-state data of a continuous culture grown at $D = 0.048$ h^{-1} ($C_X = 0.52$ g L^{-1}; $C_{nh} = 1$ mM; $C_b = 0.5$ wt %). K_M values omitted are negligibly small ($<10^{-4}$ times C or C_L). [b] See Sipkema et al. (1998c)

The NADH levels are affected by changes in the K_M values of enzymes at the branch point (FD, AS, PS) (Table 4). This way, the division of the flux over catabolism and biosynthesis (biomass, PHB) is affected, leading to changes in steady-state levels of both biomass and PHB (Table 4). As a result of the very small volume of the cells compared to that of the reactor, an additional amount of methane entering the pathway leads to a small change in biomass but to large changes in intracellular PHB and NADH concentrations (see FD, AS, and PS in Table 4). Similarly, the stoichiometric parameters α (energy used for growth) and δ (energy produced from NADH) affect the division of the flux over catabolism and biosynthesis (assimilation/dissimilation flux ratio) and thus the biomass, NADH, and PHB concentrations (Table 4).

An analysis of the influence of the various enzyme levels (V_{MAX} values) on the flux of methane through the central pathway ($q_{MO}C_X$ [mol L^{-1} s^{-1}]) supports these

Table 4. Sensitivity Analysis of the Affinity Constants and Stoichiometric Parameters of the Growth Model of *M. trichosporium* OB3b[a]

enzyme system	parameter C_X − [%]	C_X + [%]	C_{nh} − [%]	C_{nh} + [%]	C_b − [%]	C_b + [%]
Affinity Constants						
sMMO						
$K_{M,MO,m}$	−0.8	+0.8	*b*	*b*	−0.1	+0.1
$K_{M,MO,nh}$	−0.1	+0.1	*b*	*b*	*b*	*b*
$K_{M,MO,o}$	−0.2	+0.2	*b*	*b*	*b*	*b*
FD						
$K_{M,FD,fd}$	+1.7	−0.3	−30	+20	−290	+70
AS						
$K_{M,AS,fd}$	−0.3	+1.4	+22	−27	+70	−240
$K_{M,AS,nh}$	−0.2	+0.3	+9.5	−9.1	+40	−60
PS						
$K_{M,PS,nh}$	+0.4	−0.3	+0.9	−0.5	−65	+35
Stoichiometric Constants						
α	−7.6	+6.7	−31	+18	−300	+64
δ	+9.1	−7.0	+23	−14	+74	−250

[a] Percentage change in steady-state biomass, NADH, and PHB concentrations resulting from −10% and +10% change in parameter. Standard values see Tables 2 and 3 and $C_X = 0.52$ g L^{-1}; $C_{nh} = 1$ mM; $C_b = 0.5$ wt %. The effect on K_M parameters not shown was negligible. [b] These influences were negligible (<0.05%).

observations. The first enzyme of the pathway (sMMO) is the most sensitive and primarily controls the flux (87%), while the remaining influence stems from the enzymes at the branch point: FD 5%, AS 5%, and PS 3%. Flux control at the first enzyme (sMMO) prevents the energy-consuming conversion of growth substrate unless it is properly utilized by the organism for biosynthesis.

Parameter Estimation from Steady-State Measurements. Since for the sensitive parameters of sMMO literature values are available (Table 2), nine organism-specific parameters that influence the steady-state are unknown (see Table 4: four K_M values of FD, AS, and PS, and α and δ; and the V_{MAX} values of FD, AS, and PS). In practice, this number is lower, since the V_{MAX} and K_M values of the same enzyme system are not independent (a single rate is calculated).

In steady-state, the model consists of mass balance equations for 11 compounds (Table 1), containing 11 initially unknown steady-state concentrations. However, since measurements of a continuous culture provide information concerning three of the concentrations (biomass, NADH, and PHB), three organism-specific parameters are known (e.g., α, $V_{MAX,AS}$, and $V_{MAX,PS}$). Because the experimental data are used for fitting, it follows that the model gives an exact representation of the measured steady state. The estimation of one of the parameters, α, deserves more attention.

Assuming the degradation rate of PHB to be negligible (*6*), which seems fair from an energetic point of view, the steady-state yield of biomass on methane provides the assimilation/dissimilation flux ratio. A combination of this information with the steady-state mass balance of NADH leads to a relation between α and δ. So, by fixing either one of these parameters, depending on the information available, the other can be calculated. Note that the two parameters are not independent, since in the model a too-high value for α (too much energy used for biomass synthesis) can be compensated for by a higher value for δ (more energy produced from NADH). Thus, different sets of α−δ values can give similar results. In the model for strain OB3b, we fixed δ at the common value of 2 (the theoretical maximum is 3). An alternative

would be to use a theoretical α value, which is available for a range of substrates (the Y_{ATP} concept) (*18*, *40*−*43*). However, for strain OB3b, the Y_{ATP} concept may not be useful, because methylotrophs are believed to be NAD(P)H-limited rather than ATP-limited (*44*, *45*).

With $\delta = 2$, the following three parameters were estimated on the basis of steady-state measurements: $\alpha = 12$, $V_{MAX,AS} = 3.3$ mol s^{-1} kg^{-1}, and $V_{MAX,PS} = 1.4\ 10^{-3}$ mol s^{-1} kg^{-1}.

Sensitivity Analysis for Transient-State Conditions. ***Role of NADH.*** Model calculations showed that the value of the affinity constant of NADH for growth ($K_{M,AS,nh}$) influences the time needed, starting from a relatively small inoculum, to reach steady state. In the model, NADH links the enzyme steps into a chain (see Figure 1) and steers the concentrations in the direction of steady-state with a rate depending on the K_M values. A large value of the affinity constant of NADH for growth ($K_{M,AS,nh}$) relative to the NADH concentration and so a strong control by NADH appeared to correlate with a small time period. Also, a minimal affinity ($K_{M,AS,nh} > 0.1C_{nh}$), i.e., a minimal control by NADH, appeared to be necessary to obtain a stable and well-regulated model. Otherwise, the enzyme steps are not sufficiently linked. This regulatory role of NADH, as well as the influence of its concentration on the assimilation/dissimilation flux ratio discussed above, probably is realistic because others also noted this experimentally (*32*, *46*−*49*).

Regulation of Biomass Synthesis. Depending on the model values of the affinity constants for growth ($K_{M,AS}$ parameters), biomass synthesis (q_{AS}) can be controlled either by formaldehyde ($K_{M,AS,fd} \gg C_{fd}$) and/or by NADH ($K_{M,AS,nh} \gg C_{nh}$) (see eq A-5 in the appendix, oxygen is available in excess). In general, high energy levels and thus high NADH concentrations are expected to increase the assimilation rate, leading to additional NADH consumption and lowering of the NADH levels. Conversely, low energy and NADH levels will inhibit the assimilation and induce the dissimilation, leading to an increase in NADH levels.

As discussed above, a certain amount of control by NADH ($K_{M,AS,nh} > 0.1C_{nh}$) is necessary to obtain a stable and well-regulated growth model. The degree of control by formaldehyde and/or NADH is directly coupled to the ability of a cell to instantaneously increase its growth rate (μ) in response to an increase in flux through the central pathway. If neither formaldehyde nor NADH controls growth, it is limited by the growth-related enzyme levels ($V_{MAX,AS}$ value). Hence, the cells cannot grow at a rate higher than that dictated by the dilution rate ($V_{MAX,AS} = \mu/Y_{Xfd}$, with $\mu = D$ and Y_{Xfd} the yield of biomass on formaldehyde). Only after induction of these enzymes (increase in $V_{MAX,AS}$) can a higher growth rate be reached. This situation, where PHB is used as a buffer for growth substrate, has recently been proposed to be common to many microorganisms (*16*). On the other hand, if the activity of the growth-related enzymes is sufficiently large and thus formaldehyde and NADH do control growth, the cells can instantaneously increase their growth rate up to the maximum value ($V_{MAX,AS} \geq \mu_{MAX}/Y_{Xfd}$). Then, PHB does not need to function as a buffer for growth substrate.

Simulations of a methanol pulse (0.05 mM) added to a continuous culture of strain OB3b, assuming different types of growth control, i.e., (1) neither formaldehyde nor NADH ($C_{fd} \gg K_{M,AS,fd}$ and $C_{nh} \gg K_{M,AS,nh}$); (2) formaldehyde only ($K_{M,AS,fd} \gg C_{fd}$ and $C_{nh} \gg K_{M,AS,nh}$); (3) NADH only ($C_{fd} \gg K_{M,AS,fd}$ and $K_{M,AS,nh} \gg C_{nh}$); and (4) both formaldehyde and NADH ($K_{M,AS,fd} \gg C_{fd}$ and $K_{M,AS,nh} \gg C_{nh}$), clearly illustrate these effects. With neither NADH nor formaldehyde controlling growth rate, NADH levels respond strongly (Figure 2A), no additional biomass is formed (Figure 2B), and all additional methanol is converted to PHB (Figure 2C). Correspondingly, the oxygen consumption is very low (Figure 2D), because PHB is a very reduced compound, and formation of it involves far less ATP and thus oxygen consumption than does biomass formation. With growth control by formaldehyde and more importantly by NADH, NADH levels react less ("are better controlled") (Figure 2A), and increasing amounts of biomass are formed (Figure 2B). Correspondingly, decreasing amounts of PHB are formed (Figure 2C), and increasing amounts of oxygen are consumed (Figure 2D). Note that the relative change in biomass concentration (<0.1%, Figure 2B) is far smaller than the corresponding change in PHB concentration (>10%; Figure 2C) as was seen in the steady-state sensitivity analysis discussed above (Table 4). Thus, if the experimental response of a culture to a pulse injection of methanol is available, it is possible to analyze the type of growth control of the cells with the model.

Parameter Estimation from Transient-State Measurements. Apart from insight in the dynamic behavior of the model, the simulations discussed (Figure 2) illustrate the sensitivity of the parameters of growth (AS) during methanol pulses. Of the variables shown in Figure 2A−D, the dissolved oxygen concentration is the most suitable for parameter estimation, because it is very sensitive, provides much information about the metabolic state of the cell, and can easily be measured on-line without disrupting the culture. Therefore, experimental dissolved oxygen data from selected transient-state experiments were used to estimate the remaining unknown parameters (Table 3). The parameters describing the degradation rate of PHB (PD), which do not play a role in the experiments discussed here, were estimated from experiments conducted under NADH limiting conditions and are discussed elsewhere (*12*).

Since not all parameters are equally sensitive in the different types of transient-state experiments, although all parts of the model are intimately linked via NADH, initial estimations were based on one type of experiment only (gas block, methanol pulse, formaldehyde pulse, formate pulse; see Table 3). However, eventually the set of parameters was determined (Table 3) that described the complete set of experimental data most accurately (Figure 3). Because there are more fitted parameters than independent variables, the parameter set obtained is not unique. It is useful though, because it describes a large set of experiments. Furthermore, it should be noted that (1) all values fall within ranges given in the literature for similar enzymes (not shown); (2) different types of experiments were used, each triggering another enzymatic step; (3) the number of experiments used (seven) is larger than the number of metabolic steps containing estimated parameters (six: MD, AS, FD, PS, IN, M); and (4) in each experiment the whole range of substrate concentrations, from excess ($C \gg K_M$) to limitation ($C \ll K_M$), was covered, thus effectively probing the kinetic behavior of the enzyme.

As a check on the sMMO parameters obtained from literature (Table 2) and to determine the kinetic parameters of maintenance (Table 3) for the chemostat considered, a gas block experiment (Figure 3A) was used. Because this culture was grown at $\mu = 60\%\ \mu_{MAX}$, maintenance was assumed to play a role only after the

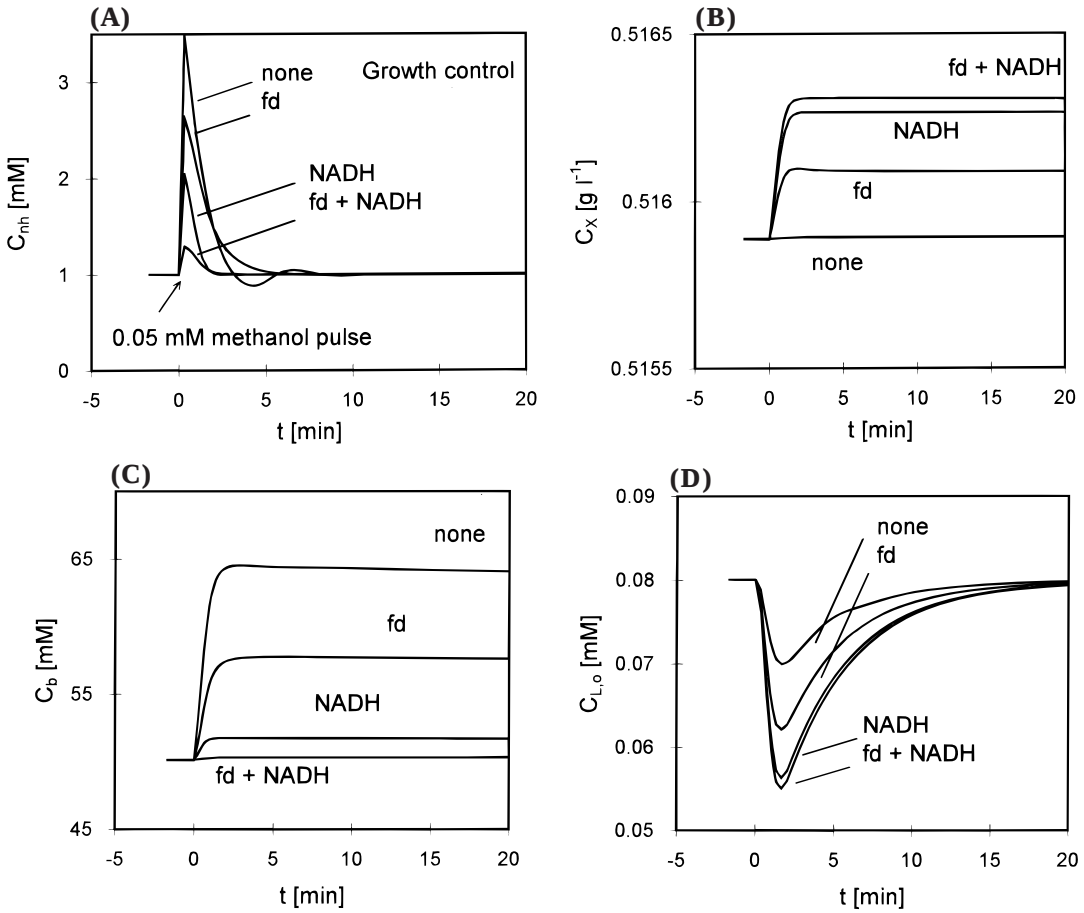

Figure 2. Effect of biosynthesis regulation on the response to a methanol pulse. Calculations with the model for strain OB3b describing growth on methane in a continuous culture ($C_X = 0.52$ g L^{-1}; $C_{nh} = 1$ mM; $C_b = 0.5$ wt %; $D = 0.048$ h^{-1}). Different types of growth control are assumed: neither NADH nor formaldehyde (none), either NADH (NADH) or formaldehyde (fd), or both NADH and formaldehyde (fd + NADH) (for details, see text). Shown are simulations of the responses to a 0.05 mM methanol pulse ($t = 0$) in (A) NADH, (B) biomass, (C) PHB, and (D) dissolved oxygen concentrations.

methane supply was switched off ($t > 0$). From the maximum maintenance coefficient obtained ($M = 5.0 \times 10^{-4}$ mol s^{-1} kg^{-1}), a maximum biomass decay rate was calculated using a conversion factor of 1.4 kg of O_2 per kg of biomass. This rate (0.48 d^{-1}), as well as the rate under the experimental conditions (≈ 0.2 h^{-1}, calculated from q_M, see appendix eq A-11, Figure 3A and Table 3), compares well with literature values found for other organisms (*50*, *51*).

Methanol pulsing (Figure 3B) was used to estimate the kinetic parameters of methanol dehydrogenase (Table 3) and, together with formaldehyde and formate pulsing (Figure 3C, 3D), those of the enzyme systems at the branch point (Table 3). In addition, the formate pulses were used to estimate the parameters of the transport equation (IN, Table 3).

Model Validation. The model was validated by comparing experimental data with model simulations using the standard set of parameters (Tables 2 and 3). It appeared that the model gave a realistic description of a gas block and of various substrate pulse experiments performed with the same culture (culture I) as used for fitting. Also with another culture (II) grown at the same rate (see, e.g., Figure 4A; for an overview of the validation experiments see Table 5) a good description was obtained. Without changing the kinetic parameters, similar results were obtained for a culture grown at a lower rate (culture III, $D = 0.024$ h^{-1}) (Figure 4B, 4C; Table 5). However, because in this case a lower yield was obtained (0.3 g g^{-1} instead of 0.4 g g^{-1}), the value of α had to be adapted. Both yield values fall within the range of published values though (0.2−0.7 g g^{-1} (*45*)).

The model was again tested with a different type of transient-state experiment. In a continuous culture growing at $D = 0.024$ h^{-1} (culture III, Table 5), during 40 min methanol (25 or 50 mM) was added via the liquid inlet. Without further adaptations in parameter values, responses not only in dissolved oxygen (Figure 5A) but also in PHB (Figure 5B) and outlet methane concentrations (Figure 5C) were described realistically. The response in oxygen and PHB levels of culture III subjected to a 1 mM formate pulse appeared to be very similar to that of the methanol step experiments and was found to be equally well-described by the model (experimental results not shown, but similar to Figure 5). In this case also NADH levels were measured. They appeared to increase from 1 mM (steady-state value) to around 3 mM, a response in accordance with model predictions.

The surprisingly good performance of the growth model in describing various steady-state and transient-state situations indicates that growth of strain OB3b is probably NAD(P)H-limited rather than ATP-limited. Anthony (*44*) suggests that this is true for many methylotrophs. If OB3b grows NAD(P)H-limited, this cofactor will play a regulatory role, as it does in the model.

Model Application. *Cofactor PQQH.* During conversion of methanol by methanol dehydrogenase, the cofactor PQQH, which enters the electron transport chain at the level of cytochrome *c*, is consumed. Although this implies a maximal energy production of only 1 ATP, as

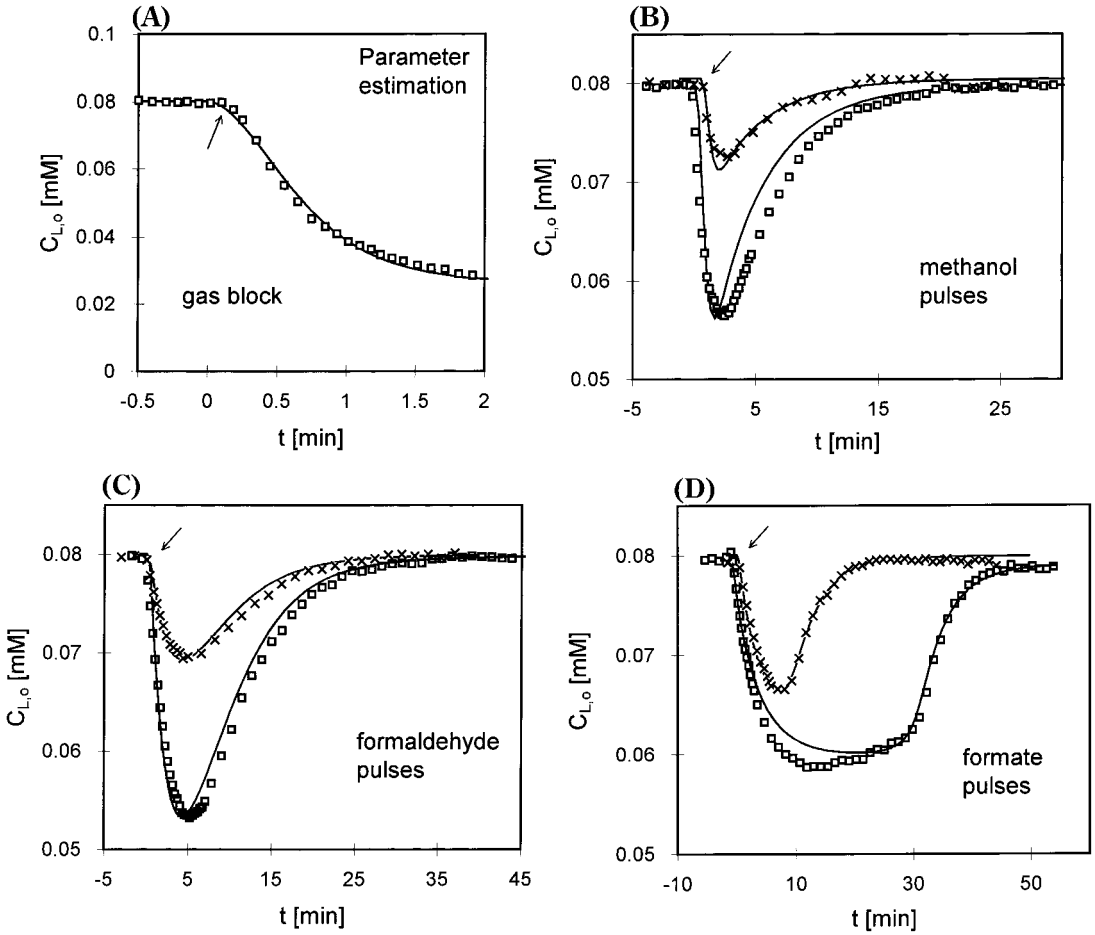

Figure 3. Transient-state experiments used for estimation of parameters of the model for strain OB3b. Comparison of experimental results with a model simulation using the set of parameters of Tables 2 and 3. Experiments were performed in a continuous culture growing on methane (C_X = 0.52 g L^{-1}; C_{nh} = 1 mM; C_b = 0.5 wt %; D = 0.048 h^{-1}). Shown are responses in dissolved oxygen levels for the following experiments, performed at t = 0 (↓): (A) a gas block (□); (B) methanol pulses of 0.017 mM (×) and 0.047 mM (□); (C) formaldehyde pulses of 0.057 mM (×) and 0.15 mM (□); and (D) formate pulses of 0.20 mM (×) and 0.86 mM (□); (—) = model.

Table 5. Overview of the Transient-State Experiments Used for the Validation of the Model for Growth of *M. trichosporium* Strain OB3b

continuous culture	D [h^{-1}]	type of experiment	size pulse/step [mM]	measured concentration
I	0.048	formaldehyde pulse	0.41	$C_{L,o}$
II	0.048	gas block		$C_{L,o}$
		methanol pulse	0.069, 0.21	$C_{L,o}$
		formate pulse	0.82	$C_{L,o}$
III	0.024	gas block		$C_{L,o}$
		methanol pulse	0.029, 0.051, 0.073, 0.083	$C_{L,o}$
		formate pulse	0.27, 0.52, 0.72, 0.97	$C_{L,o}$
			1.0	$C_{L,o}$, C_b, C_{nh}, $C_{G,m}$
		methanol step	25	$C_{L,o}$
			50	$C_{L,o}$, C_b, $C_{G,m}$

opposed to 3 per NADH, in the model both cofactors are assumed to produce the same amount of energy. If this discrepancy is incorporated in the model (PQQH = 0.33NADH), the stoichiometric equation of methanol dehydrogenase (eq 2) changes, as does the NADH balance and thus the value of α since it is calculated from steady-state measurements (see above). Although this leads to a large change in α, from 12 down to 6.7, methanol conversion kinetics are hardly affected (Figure 6). So, the model is not sufficiently refined to warrant distinction between NADH and PQQH, which justifies our simplifying assumption. Note that the theoretical α value (Y_{ATP}) of 8.3, estimated on the basis of information provided by Anthony (*44*) and Leak and Dalton (*41*), is between our calculated values of 6.7 (1 ATP per NADH) and 12 (3 ATP per NADH).

Regulation of Growth by Strain OB3b. An analysis of the values estimated for the affinity constants for growth ($K_{M,AS,nh}$, $K_{M,AS,fd}$, Table 3) implies that in strain OB3b NADH controls growth ($K_{M,AS,nh} \approx C_{nh}$), but formaldehyde does not ($C_{fd} \gg K_{M,AS,fd}$). Furthermore, the V_{MAX} value for growth ($V_{MAX,AS} \approx \mu_{MAX}/Y_{Xfd}$) indicates that strain OB3b can instantaneously increase its growth rate up to the maximum value in response to an increase in carbon flux through the main pathway. Thus, the V_{MAX} for growth does not appear to be adapted in response to continued growth at a low rate. Since the activities of the other enzymes of the metabolic pathway are not adapted either, i.e., the same V_{MAX} values describe different growth rates, strain OB3b appears to have a "rigid enzyme system". A similar conclusion can be drawn from a comparison of the calculated and published μ_{MAX}

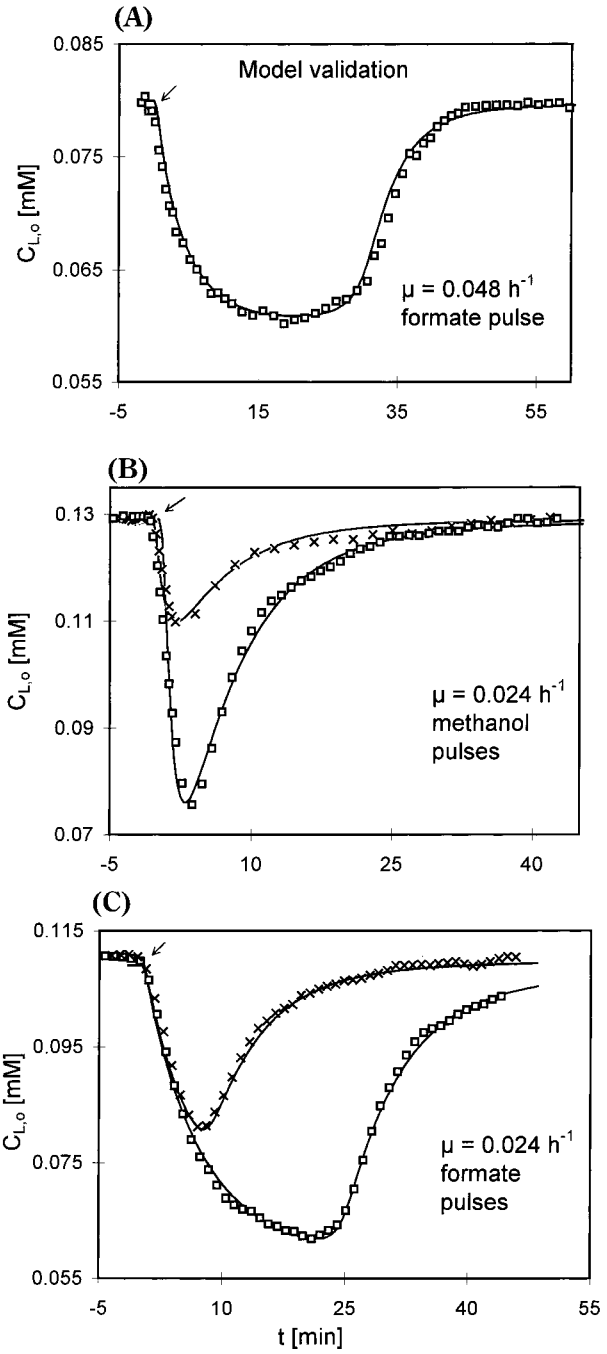

Figure 4. Pulse experiments used for the validation of the model for strain OB3b. Response in dissolved oxygen concentration as a function of time. At $t = 0$ (↓), a substrate pulse was injected in a continuous culture growing on methane. Shown are (A) a formate pulse of 0.82 mM (□) injected in culture II ($C_X = 0.51$ g L^{-1}; $D = 0.048$ h^{-1}); (B) methanol pulses of 0.029 mM (×) and 0.073 mM (□) injected in culture III ($C_X = 0.64$ g L^{-1}; $D = 0.024$ h^{-1}); and (C) formate pulses of 0.27 mM (×) and 0.97 mM (□) injected in culture III; (—) = model.

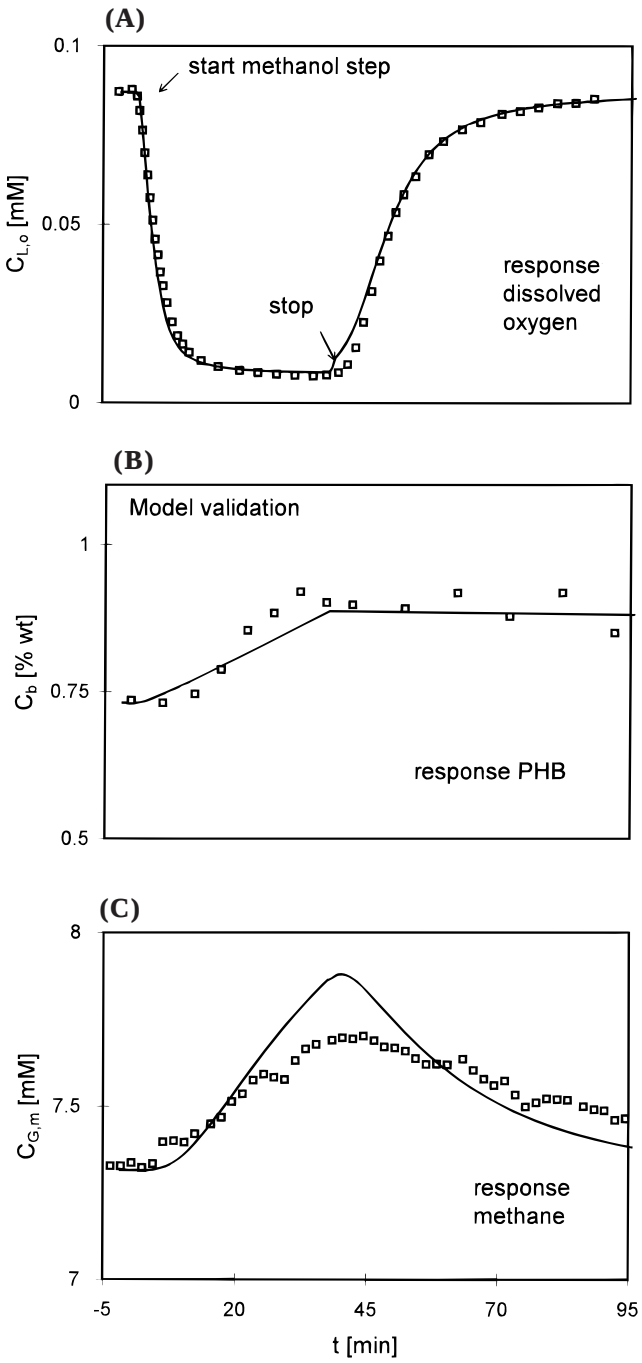

Figure 5. Step experiment used for the validation of the model for strain OB3b. At $t = 0$, the methanol inlet concentration of continuous culture III growing on methane ($C_X = 0.64$ g L^{-1}; $D = 0.024$ h^{-1}) is changed stepwise from 0 to 50 mM. Shown are responses in (A) dissolved oxygen, (B) PHB, and (C) outlet methane concentration, as a function of time; (□) = experimental results, (—) = model.

values: 0.085 h^{-1} (α adapted for low yield) and 0.13 h^{-1} (standard α) (model), and 0.08−0.085 h^{-1} (literature) (*52*, *53*).

PHB Metabolism. The storage material PHB accumulates during periods of unbalanced growth. Most studies focused on accumulation under conditions of sustained nitrogen, phosphorus, or oxygen limitation, but it may also occur during short periods of excess carbon source availability after growth under carbon limitation (*7*, *54*).

In our study with strain OB3b, the first indication of involvement of PHB or a similar NADH buffer in the metabolism of the cells came from a model analysis of the oxygen consumption pattern observed after injection of a pulse of formate in a continuous culture. It appeared that the experimental data could only be properly described by assuming a buffer for NADH to be present. If all additional NADH produced as a result of formate conversion were immediately used for growth, initially far more oxygen should have been consumed than observed experimentally (Figure 7).

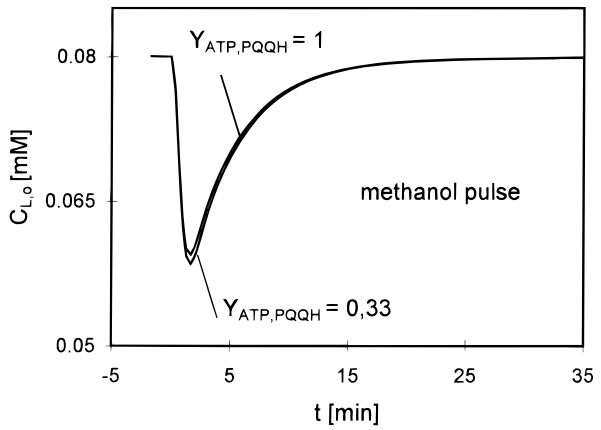

Figure 6. Effect of different model assumptions concerning the cofactor PQQH of methanol dehydrogenase. Calculations with the model for strain OB3b, influence of the yield of ATP resulting from conversion of PQQH in the electron transport chain ($Y_{ATP,PQQH}$). Shown is the response in dissolved oxygen concentration to a 0.04 mM methanol pulse (t = 0), injected in a continuous culture growing on methane, as a function of time. Assumptions: PQQH = NADH ($Y_{ATP,PQQH}$ = 1) and PQQH = 0.33NADH ($Y_{ATP,PQQH}$ = 0.33). Parameter values as in Tables 2 and 3, with α = 6.7 for the PQQH = 0.33 NADH simulation.

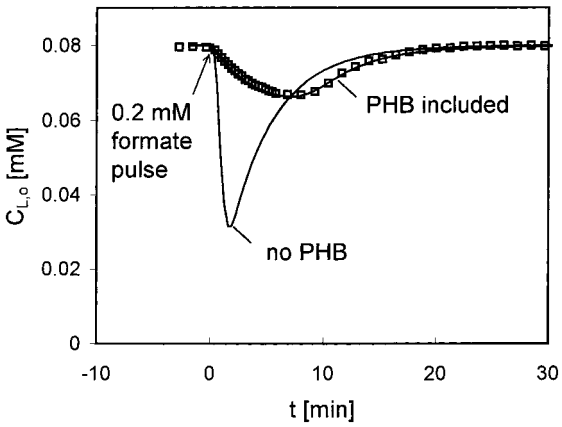

Figure 7. Effect of incorporation of PHB metabolism in the model for strain OB3b. Response in dissolved oxygen levels following a pulse injection of formate (t = 0, 0.20 mM) into a continuous culture growing on methane (C_X = 0.52 g L^{-1}; C_{nh} = 1 mM; C_b = 0.5 wt %; D = 0.048 h^{-1}). Simulations are shown both with the standard model and with a model that does not include a NADH buffer like PHB.

In further transient-state experiments (large formate pulse, methanol step), a PHB accumulation was observed (see, e.g., Figure 5B), substantiating our initial conclusion. The knowledge that in strain OB3b PHB plays a role as a buffer for transiently available excess reducing power may be useful for practical purposes, for example, to improve processes involving cometabolic conversions. By ensuring the presence of sufficient PHB and thus of reducing power, it is expected that long-term cometabolic contaminant conversion under starvation conditions is enhanced. Experimental results, obtained both with mixed cultures of methanotrophs (*55*−*57*) and with strain OB3b (*58*) verify this hypothesis.

Conclusions

A metabolic model was developed to study growth of *M. trichosporium* OB3b on methane in continuous culture. The model consists of a set of ordinary differential equations (time-dependent mass balances) that incorporate stoichiometry based on the metabolic pathways and Michaelis−Menten type enzyme kinetics. The cofactor NADH, which is assumed to be in equilibrium with the energy carrier ATP via oxidative phosphorylation, links the metabolic steps, thus acting as a central intermediate and regulating factor. Model parameters were either obtained from literature, determined in independent batch experiments, or fitted from steady-state or transient-state measurements.

The model could be validated by additional transient-state experiments in which oxygen, methane, PHB, and NADH were measured. It appeared that by incorporating NADH as a central and controlling intermediate, a stable and well-regulated model was obtained that gives a realistic description of a variety of steady-state and transient-state experimental data. Steady-state model calculations prove flux control in strain OB3b to be located primarily at the first enzyme of the metabolic pathway (sMMO) and to a lesser extent at the enzymes at the branch point between catabolism, PHB metabolism, and growth.

Both transient-state and μ_{MAX} calculations reveal that strain OB3b has a "rigid enzyme system", the activity of which is not adapted in response to continued low growth rates (30% μ_{MAX}). The storage material PHB, which was found to accumulate after pulses of formate and during step changes in inlet methanol concentration, functions as a sink for transiently available excess reducing power.

The presented model is suitable to develop and optimize processes in which NADH plays a crucial role, such as in cometabolic conversions. Also, because it is based directly on available knowledge of the biochemical processes involved, it can be used to gain insight in the cells' metabolism as illustrated by the examples discussed.

Notation

Abbreviations and Subscripts

ADP	adenosine diphosphate
AS	assimilation (growth)
ATP	adenosine triphosphate
b	PHB
EX	cellular membrane transport, directed extracellularly
fd	formaldehyde
FD	formaldehyde dehydrogenase
ft	formate
FT	formate dehydrogenase
HY	dehydration reaction formaldehyde
in	in the ingoing flow
IN	cellular membrane transport, directed intracellularly
o	oxygen
m	methane
MD	methanol dehydrogenase
ml	methanol
MO	soluble methane monooxygenase (sMMO)
n(h)	NAD(H)
NAD(H)	nicotinamide adenine dinucleotide (reduced/oxidized form)
n_{tot}	= NAD + NADH
PS	PHB synthesis
PD	PHB degradation
PHB	poly-β-hydroxybutyric acid
PQQ(H)	pyrrolo-quinoline quinone (reduced/oxidized form)
sMMO	soluble methane monooxygenase
wt %	% cell dry weight

Symbols

C_j	intracellular concentration of compound j [mol L^{-1}]
$C_{L,j}$	liquid concentration of compound j (averaged over extra- and intracellular) [mol L^{-1}]
$C_{G,j}$	gas-phase concentration of compound j [mol L^{-1}]
C_X	biomass concentration [kg L^{-1}]
D	dilution rate (liquid flow/volume) [s^{-1}]
k_{HY}	first-order rate constant of formaldehyde dehydration reaction [s^{-1}]
$K_{EQ,fd}$	equilibrium constant of dehydration reaction of formaldehyde ($= C_{fd}/C_{L,fd}$)
$K_{EQ,ft}$	equilibrium constant of transport reaction of formate ($= C_{ft}/C_{L,ft}$)
$K_{I,PD,nh}$	NADH-related inhibition constant for PHB degradation [mol L^{-1}]
$K_{I,PD,MAX}$	maximum $K_{I,PD,nh}$ leading to minimal inhibition by NADH [mol L^{-1}]
$K_{I,PD,MIN}$	minimum $K_{I,PD,nh}$ leading to maximal inhibition by NADH [mol L^{-1}]
$K_{I,PD,SP}$	set point below which PHB breakdown is enhanced [mol L^{-1}]
$K_{M,i,j}$	affinity of enzyme system i for compound j [mol L^{-1}]
M	maximum rate of energy (mol NADH) consumption for maintenance [mol s^{-1} kg^{-1}]
p	power in Hill equation
q_i	specific conversion rate of enzyme system i [mol s^{-1} kg^{-1}]
v_{HY}	rate of formaldehyde dehydration reaction [mol s^{-1} L^{-1}]
V_L	liquid volume [L]
$V_{MAX,i}$	maximum rate of enzyme system i [mol s^{-1} kg^{-1}]
w	power in Hill equation
Y_{ATP}	$= \alpha$
$Y_{ATP,PQQH}$	yield of ATP resulting from conversion of PQQH in the electron transport chain
Y_{Xfd}	growth yield of biomass on formaldehyde [kg mol^{-1}]

Greek Symbols

α	amount of energy (mol ATP) used per C-mole of biomass formed
δ	(= P/O ratio), energy (mol ATP) produced per atom of oxygen used in oxidative phosphorylation
μ, μ_{MAX}	(maximum) specific growth rate [s^{-1}]

Acknowledgment

The authors thank the students J. Krijnen, G. Ragetlie, M. Segers, and C. Schmidt for carrying out parts of the experimental program, the Kluyver Laboratory in Delft for the PHB analyses, and Professor J. J. Heijnen for critical comments on the manuscript.

Appendix

Summary of the kinetic equations incorporated in the model for growth of *M. trichosporium* OB3b on methane:

$$q_{MO} = V_{MAX,MO}\left(\frac{C_{L,m}}{C_{L,m} + K_{M,MO,m}}\right)\left(\frac{C_{nh}}{C_{nh} + K_{M,MO,nh}}\right)\left(\frac{C_{L,o}}{C_{L,o} + K_{M,MO,o}}\right) \quad \text{(A-1)}$$

$$q_{MD} = V_{MAX,MD}\left(\frac{C_{L,m}}{C_{L,m} + K_{M,MD,ml}}\right)\left(\frac{C_n}{C_n + K_{M,MD,n}}\right) \quad \text{(A-2)}$$

$$q_{FD} = V_{MAX,FD}\left(\frac{C_{fd}}{C_{fd} + K_{M,FD,fd}}\right)\left(\frac{C_n}{C_n + K_{M,FD,n}}\right) \quad \text{(A-3)}$$

$$V_{HY} = k_{HY}(K_{EQ,fd}C_{L,fd} - C_{fd}) \quad \text{(A-4)}$$

$$q_{AS} = V_{MAX,AS}\left(\frac{C_{fd}}{C_{fd} + K_{M,AS,fd}}\right)\left(\frac{C_{nh}}{C_{nh} + K_{M,AS,nh}}\right)\left(\frac{C_{L,o}}{C_{L,o} + K_{M,AS,o}}\right) \quad \text{(A-5)}$$

$$q_{PS} = V_{MAX,PS}\left(\frac{C_{fd}}{C_{fd} + K_{M,PS,fd}}\right)\left(\frac{C_{nh}^p}{C_{nh}^p + K_{M,PS,nh}^p}\right) \quad \text{(A-6)}$$

$$q_{PD} = V_{MAX,PD}\left(\frac{C_b}{C_b + K_{M,PD,b}}\right)\left(\frac{C_n}{C_n + K_{M,PD,n}}\right)\left(\frac{C_{L,o}}{C_{L,o} + K_{M,PD,o}}\right)\left(\frac{1}{1 + C_{nh}/K_{I,PD,nh}}\right) \quad \text{(A-7)}$$

$$K_{I,PD,nh} = K_{I,PD,MAX}\left(1 - \frac{C_{nh}^w}{C_{nh}^w + K_{M,PD,SP}^w}\right) + K_{I,PD,MIN}\left(\frac{C_{nh}^w}{C_{nh}^w + K_{M,PD,SP}^w}\right) \quad \text{(A-8)}$$

$$q_{FT} = V_{MAX,FT}\left(\frac{C_{ft}}{C_{ft} + K_{M,FT,ft}}\right)\left(\frac{C_n}{C_n + K_{M,FT,n}}\right) \quad \text{(A-9)}$$

$$q_{IN} = \frac{V_{MAX,IN}(C_{L,ft}C_{ft}/K_{EQ,ft})}{C_{L,ft} + K_{M,IN} + K_{M,IN}C_{ft}/K_{M,EX}} \quad \text{(A-10)}$$

$$q_M = M\left(\frac{C_{nh}}{C_{nh} + K_{M,M,nh}}\right)\left(\frac{C_{L,o}}{C_{L,o} + K_{M,M,o}}\right) \quad \text{(A-11)}$$

References and Notes

(1) Harrison, D. E. F.; MacLennan, D. G.; Pirt, S. J. Responses of bacteria to dissolved oxygen tension. In *Fermentation Advances*; Perlman, D., Ed.; Academic Press: New York and London, 1969; pp 117−144.

(2) Hess, B.; Boiteux, A. Mechanism of glycolytic oscillation in yeast, I. *Hoppe-Seyler's Z. Physiol. Chem.* **1968**, *349*, 1567−1574.

(3) Hommes, F. A. Oscillatory reductions of pyridine nucleotides during anaerobic glycolysis in brewers' yeast. *Arch. Biochem. Biophys.* **1964**, *108*, 36−46.

(4) Matin, A.; Gottschal, J. C. Influence of dilution rate on NAD(P) and NAD(P)H concentrations and ratios in a *Pseudomonas* sp. grown in continuous culture. *J. Gen. Microbiol.* **1976**, *94*, 333−341.

(5) Wimpenny, J. W. T.; Firth, A. Levels of nicotinamide adenine dinucleotide and reduced nicotinamide adenine dinucleotide in facultative bacteria and the effect of oxygen. *J. Bacteriol.* **1972**, *111*, 24−32.

(6) Dawes, E. A.; Senior, P. J. The role and regulation of energy reserve polymers in microorganisms. In *Advances in Microbial Physiology*; Rose, A. H., Tempest, D. W., Eds.; Academic Press: London and New York, 1973; pp 135−266.

(7) de Haan, A.; Smith, M. R.; Voorhorst, W. G. B.; de Bont, J. A. M. Cofactor regeneration in the production of 1,2-epoxypropane by *Mycobacterium* strain E3: the role of storage material. *J. Gen. Microbiol.* **1993**, *139*, 3017−3022.

(8) Ko, Y. F.; Bentley, W. E.; Weigand, W. A. An integrated metabolic modeling approach to describe the energy efficiency of *E. coli* fermentations under oxygen-limited conditions:

Cellular energetics, carbon flux, and acetate production. *Biotechnol. Bioeng.* **1993**, *42*, 843−853.
(9) Mankad, T.; Nauman, E. B. Effect of oxygen on steady-state product distribution in *Bacillus polymyxa* fermentations. *Biotechnol. Bioeng.* **1992**, *40*, 413−426.
(10) Rapoport, T. A.; Heinrich, R.; Rapoport, S. M. The regulatory principles of glycolysis in erythrocytes in vivo and in vitro. A minimal comprehensive model describing steady states, quasi-steady states and time-dependent processes. *Biochem. J.* **1976**, *154*, 449−469.
(11) Weusthuis, R. A.; Adams, H.; Scheffers, W. A.; van Dijken, J. P. Energetics and kinetics of maltose transport in *Saccharomyces cerevisiae*: a continuous culture study. *Appl. Environ. Microbiol.* **1993**, *59*, 3102−3109.
(12) Sipkema, E. M.; de Koning, W.; Ganzeveld, K. J.; Janssen, D. B.; Beenackers, A. A. C. M. NADH regulated metabolic model for growth of *Methylosinus trichosporium* OB3b. Incorporation of trichloroethene degradation and model application. *Biotechnol. Prog.* **2000**, *16*, 189−198.
(13) Sipkema, E. M.; de Koning, W.; Ganzeveld, K. J.; Janssen, D. B.; Beenackers, A. A. C. M. Experimental pulse technique for the study of microbial kinetics in continuous culture. *J. Biotechnol.* **1998**, 64, 159−176.
(14) Sipkema, E. M.; de Koning, W.; van Hylckama Vlieg, J. E. T.; Ganzeveld, K. J.; Janssen, D. B.; Beenackers, A. A. C. M. Trichloroethene degradation in a two-step system by *M. trichosporium* OB3b. Optimization of system performance: use of formate and methane. *Biotechnol. Bioeng.* **1998**, 63, 56−67.
(15) Degelau, A.; Scheper, T.; Bailey, J. E.; Guske, C. Fluorometic measurement of poly-β-hydroxybutyrate in *Alcaligenes eutrophus* by flow cytometry and spectrofluorometry. *Appl. Microbiol. Biotechnol.* **1995**, *42*, 653−657.
(16) van Aalst-van Leeuwen; M. A.; Pot, M. A.; van Loosdrecht, M. C. M.; Heijnen, J. J. Kinetic modeling of poly(β-hydroxybutyrate) production and consumption by *Paracoccus pantotropha* under dynamic substrate supply. *Biotechnol. Bioeng.* **1997**, *55*, 773−782.
(17) Kashket, E. R. The proton motive force in bacteria: a critical assessment of methods. *Annu. Rev. Microbiol.* **1985**, *39*, 219−242.
(18) Anthony, C. *The Biochemistry of Methylotrophs*; Academic Press: London, 1982.
(19) Colby, J.; Dalton, H.; Whittenbury, R. Biological and biochemical aspects of microbial growth on C1 compounds. *Annu. Rev. Microbiol.* **1979**, *33*, 481−517.
(20) Higgins, I. J.; Best, D. J.; Hammond, R. C.; Scott, D. Methane-oxidizing microorganisms. *Microbiol. Rev.* **1981**, *45*, 556−590.
(21) *Hydrocarbons and Methylotrophy*; Lidstrom, M. E., Ed.; Methods in Enzymology; Academic Press Inc.: San Diego, 1990; Vol. 188.
(22) Stirling, D. I.; Dalton, H. Properties of the methane monooxygenase from extracts of *Methylosinus trichosporium* OB3b and evidence for its similarity to the enzyme from *Methylococcus capsulatus* (Bath). *Eur. J. Biochem.* **1979**, *96*, 205−212.
(23) Hanson, R. S.; Hanson, T. E. Methanotrophic bacteria. *Microbiol. Rev.* **1996**, *60*, 439−471.
(24) Leak, D. J.; Dalton, H. In vivo studies of primary alcohols, aldehydes and carboxylic acids as electron donors for the methane mono-oxygenase in a variety of methanotrophs. *J. Gen. Microbiol.* **1983**, *129*, 3487−3497.
(25) Doi, Y.; Kawaguchi, Y.; Koyama, N.; Nakamura, S.; Hiramitsu, M.; Yoshida, Y.; Kimura, H. Synthesis and degradation of polyhydroxyalkanoates in *Alcaligenes eutrophus*. *FEMS Microbiol. Rev.* **1992**, *103*, 103−108.
(26) Harder, W.; Attwood, M. M.; Quayle, J. R. Methanol assimilation by *Hyphomicrobium* sp. *J. Gen. Microbiol.* **1973**, *78*, 155−163.
(27) Quayle, J. R. The metabolism of one-carbon compounds by microorganisms. In *Advances in Microbial Physiology*; Rose, A. H., Tempest, D. W., Eds.; Academic Press: London, 1972; pp 119−203.
(28) Williams, A. M. The biochemistry and physiology of poly-*beta*-hydroxybutyrate metabolism in *Methylosinus trichosporium* OB3b. Ph.D. Thesis, Cranfield Institute of Technology, Biotechnology Centre, Cranfield, U.K., 1988.
(29) Walker, J. F. *Formaldehyde*; 3rd ed.; R. E. Krieger Publishing Company: Malabar, FL, 1964.
(30) Nielsen, J.; Villadsen, J. *Bioreaction engineering principles*; Plenum Press: New York, 1994.
(31) Roels, J. A. *Energetics and Kinetics in Biotechnology*; Elsevier Biomedical Press: Amsterdam, The Netherlands, 1983.
(32) Lee, I. Y.; Kim, M. K.; Chang, H. N.; Park, Y. H. Regulation of poly-β-hydroxybutyrate biosynthesis by nicotinamide nucleotide in *Alcaligenes eutrophus*. *FEMS Microbiol. Lett.* **1995**, *131*, 35−39.
(33) Segel, I. H. *Enzyme Kinetics. Behavior and Analysis of Rapid Equilibrium and Steady-State Enzyme Systems*; John Wiley and Sons Inc.: New York, 1975.
(34) Leaf, T. A.; Srienc, F. Metabolic modeling of polyhydroxybutyrate biosynthesis. *Biotechnol. Bioeng.* **1998**, *57*, 557−570.
(35) Oldenhuis, R.; Oedzes, J. J.; van der Waarde, J. J.; Janssen, D. B. Kinetics of chlorinated hydrocarbon degradation by *Methylosinus trichosporium* OB3b and toxicity of trichloroethylene. *Appl. Environ. Microbiol.* **1991**, *57*, 7−14.
(36) Fox, B. G.; Froland, W. A.; Jollie, D. R.; Lipscomb, J. D. Methane monooxygenase from *Methylosinus trichosporium* OB3b. In *Hydrocarbons and Methylotrophy*; Lidstrom, M. E., Ed.; Methods in Enzymology; Academic Press Inc.: San Diego, 1990; Vol. 188, pp 191−202.
(37) Green, J.; Dalton, H. Protein B of soluble methane monooxygenase from *Methylococcus capsulatus* (Bath). *J. Biol. Chem.* **1985**, *260*, 15795−15801.
(38) Jollie, D. R.; Lipscomb, J. D. Formate dehydrogenase from *Methylosinus trichosporium* OB3b. In *Hydrocarbons and Methylotrophy*; Lidstrom, M. E., Ed.; Methods in Enzymology; Academic Press Inc.: San Diego, 1990; Vol. 188, pp 331−334.
(39) Bieber, R.; Trümpler, G. Angenäherte, spektrographische Bestimmung der Hydratationsgleichgewichtskonstanten Wässriger Formaldehydlösingen. *Helv. Chim. Acta* **1947**, *30*, 1860−1864.
(40) Andrews, G. Predicting yields for autotrophic and cometabolic processes. *Appl. Biochem. Biotechnol.* **1995**, *51/52*, 329−338.
(41) Leak, D. J.; Dalton, H. Growth yields of methanotrophs. 2. A theoretical analysis. *Appl. Microbiol. Biotechnol.* **1986b**, *23*, 477−481.
(42) Stouthamer, A. H. A theoretical study on the amount of ATP required for synthesis of microbial cell material. *Antonie van Leeuwenhoek* **1973**, *39*, 545−565.
(43) van Dijken, J. P.; Harder, W. Growth yields of microorganisms on methanol and methane. A theoretical study. *Biotechnol. Bioeng.* **1975**, *17*, 15−30.
(44) Anthony, C. The prediction of growth yields in methylotrophs. *J. Gen. Microbiol.* **1978**, *104*, 91−104.
(45) Leak, D. J.; Dalton, H. Growth yields of methanotrophs. 1. Effect of copper on the energetics of methane oxidation. *Appl. Microbiol. Biotechnol.* **1986a**, *23*, 470−476.
(46) Henderson, R. A.; Jones, C. W. Poly-3-hydroxybutyrate production by washed cells of *Alcaligenes eutrophus*; purification, characterisation and potential regulatory role of citrate synthase. *Arch. Microbiol.* **1997**, *168*, 486-492.
(47) Newaz, S. S.; Hersh, L. B. Reduced nicotinamide adenine dinucleotide-activated phosphoenolpyruvate carboxylase in *Pseudomonas* MA: Potential regulation between carbon assimilation and energy production. *J. Bacteriol.* **1975**, *124*, 825−833.
(48) Schneider, J. D.; Wendlandt, K. D.; Bruehl, E.; Mirschel, G. Effecktorwirkung von sauerstoffhaltigen C1−Verbindungen bei der Kultivierung des methanotrophen Bakterienstammes GB25. *Z. Allg. Mikrobiol.* **1983**, *23*, 259−268.
(49) Zinebi, S.; Raval, G.; Petitdemange, H. Effect of oxygenation and sulfate concentration on pyruvate and lactate formation in *Klebsiella oxytoca* ZS growing in chemostat cultures. *Curr. Microbiol.* **1994**, *29*, 79−85.
(50) Bilbo, C. M.; Arvin, E.; Holst, H.; Spliid, H. Modelling the growth of methane-oxidizing bacteria in a fixed biofilm. *Water Res.* **1992**, *26*, 301−309.

(51) Chang, M.-K.; Voice, T. C.; Criddle, C. S. Kinetics of competitive inhibition and cometabolism in the biodegradation of benzene, toluene, and *p*-xylene by two *Pseudomonas* isolates. *Biotechnol. Bioeng.* **1993**, *18*, 63−80.
(52) Park, S.; Hanna, M. L.; Taylor, R. T.; Droege, M. W. Batch cultivation of *Methylosinus trichosporium* OB3b. I. Production of soluble methane monooxygenase. *Biotechnol. Bioeng.* **1991**, *38*, 423−433.
(53) Sun, A. K.; Wood, T. K. Trichloroethylene degradation and mineralization by Pseudomonads and *Methylosinus trichosporium* OB3b. *Appl. Microbiol. Biotechnol.* **1996**, *45*, 248−256.
(54) van Loosdrecht, M. C. M.; Pot, M. A.; Heijnen, J. J. Importance of bacterial storage polymers in bioprocesses. *Water Sci. Technol.* **1997**, *35*, 41−47.
(55) Chu, K. H.; Alvarez-Cohen, L. Trichloroethylene degradation by methane-oxidizing cultures grown with various nitrogen sources. *Water Environ. Res.* **1996**, *68*, 76−82.
(56) Henry, S. M.; Grbic-Galic, D. Influence of endogenous and exogenous electron donors and trichloroethylene oxidation toxicity on trichloroethylene oxidation by methanotrophic cultures from a groundwater aquifer. *Appl. Environ. Microbiol.* **1991**, *57*, 236−244.
(57) Henrysson, T.; McCarty, P. L. Influence of the endogenous storage lipid poly-β-hydroxybutyrate on the reducing power availability during cometabolism of trichloroethylene and naphthalene by resting methanotrophic mixed cultures. *Appl. Environ. Microbiol.* **1993**, *59*, 1602−1606.
(58) Shah, N. N.; Hanna, M. L.; Taylor, R. T. Batch cultivation of *Methylosinus trichosporium* OB3b: V. Characterization of poly-β-hydroxybutyrate production under methane-dependent growth conditions. *Biotechnol. Bioeng.* **1996**, *49*, 161−171.

Accepted for publication January 7, 2000.

BP9901567